

# We are IntechOpen, the world's leading publisher of Open Access books Built by scientists, for scientists

6,900

Open access books available

186,000

International authors and editors

200M

Downloads

Our authors are among the

154

Countries delivered to

TOP 1%

most cited scientists

12.2%

Contributors from top 500 universities



WEB OF SCIENCE™

Selection of our books indexed in the Book Citation Index  
in Web of Science™ Core Collection (BKCI)

Interested in publishing with us?  
Contact [book.department@intechopen.com](mailto:book.department@intechopen.com)

Numbers displayed above are based on latest data collected.  
For more information visit [www.intechopen.com](http://www.intechopen.com)



## Chapter

# Theoretical and Experimental Analysis of Structural Properties of Load-Bearing Components of Thermonuclear Tokamak Installations

*Nikolay A. Makhutov, Mikhail M. Gadenin, Sergey V. Maslov, Igor A. Razumovsky and Dmitry O. Reznikov*

## Abstract

The chapter presents the results of research carried out in Mechanical Engineering Research Institute of the Russian Academy of Sciences that were focused on validation and application of design diagrams, methods and systems for measuring stresses under the modes of Tokamak installation cooling and management of electromagnetic fields during startups. The examples of tensometric systems and results of measurements of stresses under cryogenic temperatures and strong magnetic fields as well as results of analysis of the states of stresses and strains of structurally heterogeneous components of load-bearing and conductive structures are presented. Operation conditions and limit states of Tokamak components are considered. Results of research summarized in the chapter demonstrate the correctness of the adopted design solutions, which result in a relatively low level of local stresses in the load-bearing components of the thermonuclear installations.

**Keywords:** thermonuclear installation, strength, service life, local stresses and strains, limit states

## 1. Statement of problems related to structural integrity and service life of thermonuclear installations

In the modern age, the day-to-day activities of individuals, states and the international community are all closely dependent on the existence of a reliable power supply. The main components of the power industry include energy resources, power installations and power supply systems [1, 2]. Both the global and domestic energy mixes include:

- traditional power sources which have been used for a century or more (thermal - coal, oil, gas, hydraulic, wind, solar);

- new types of energy, which have been used for several decades (nuclear, geothermal, tidal, solar battery, hydrogen, bioenergy);
- promising future energy technologies (thermonuclear, space).

The changes in the respective importance of these types of energy  $\bar{E}$  and the relative growth of global energy production  $\bar{E}$  in the 21st century are shown in **Figure 1**.

In 2020, Russia adopted a new energy strategy for the period until 2035 [1]. It focuses on the development of new and promising types of energy, with a gradual reduction in dependence on traditional types which is driven by scientific and technological advances and economic efficiency and environmental considerations.

The analysis [1–3] of the prospects for the development of energy until 2030, 2050 and 2100, the focus will be primarily on problems of a scientific, design, technological and operational nature, aimed at ensuring the safety, structural integrity and service life of power facilities [4–8]. This focus is due to the fact that trends in the extraction, production and use of energy have been significantly impacted by major accidents and disasters in the late 20th and early 21st centuries in the USSR, Russia, the USA, Norway, Mexico and China, due to technical failures in unique thermal, hydraulic and nuclear power installations, offshore oil and gas production platforms, and tankers used for the transportation of oil and liquefied natural gas. These accidents and catastrophes were caused by failures to comply with structural integrity requirements and the consequent collapse of load-bearing structures including buildings, vessels, pipelines, electric generators, turbines, and platform structures. Such accidents have resulted in tens or in some cases hundreds of deaths, as well the destruction of technical facilities and chemical pollution and radioactive contamination in surrounding areas. The resulting economic losses are estimated in  $10^9$ – $10^{11}$  US dollars. In this regard, since the 1960s, scientists, engineers and specialists from around the world have begun to pay special attention to ensuring structural integrity and preventing accidents and disasters resulting from technical failures in power facilities of all types. Moreover, fundamentally new tasks have arisen in relation to both existing nuclear energy and promising thermonuclear energy technologies. These types of energy offer new solutions to problems relating to the production, processing and use of energy resources, by virtue of the far smaller volume and mass of fuel required- 1 g of deuterium used in a thermonuclear unit produces the same amount of energy as a whole column of oil tanker wagons. Thermonuclear power, in contrast to nuclear power using thermal and fast

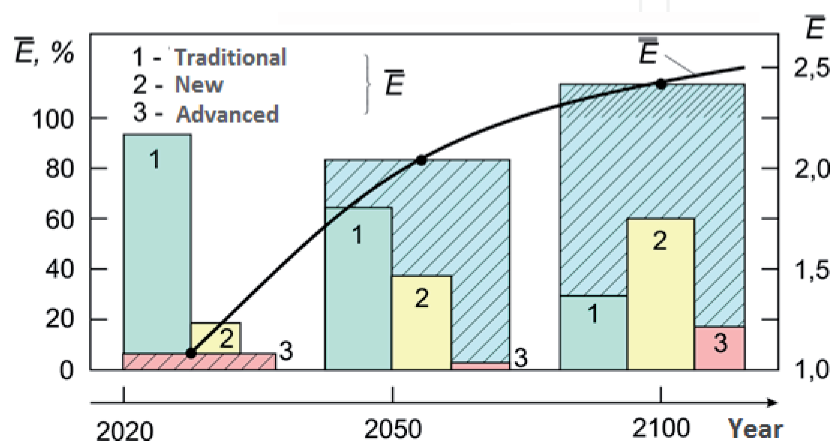


**Figure 1.**  
Structure and development potential of the energy mix.

neutrons, can fundamentally transform the risk of ionizing and radiation damage during the decay and fission of heavy uranium and plutonium nuclei.

The controlled thermonuclear fusion of deuterium-tritium and deuterium-deuterium, which was first proposed in the USSR by academicians A.D. Sakharov, I.E. Tomm and L.A. Artsimovich. This fusion results in the synthesis of heavier helium, accompanied by a release of a huge amount of energy. The thermonuclear fusion processes carried out in thermonuclear power installations on Earth are essentially the same as the processes that take place on the surface of and inside the Sun.

The subsequent theoretical research on, and practical development [2] of thermonuclear fusion in Russia was led by Academicians E.P. Velikhov, V.A. Glukhikh, and B.B. Kadomtsev, who worked on the physics of thermonuclear installations, and Academician K.V. Frolov [2]., who worked on issues relating to mechanics and the structural integrity and service life of facilities. The initial reactors developed for use in thermonuclear installations were of two types:

- pulsed reactors in which small targets with a deuterium-tritium ( $D-T$   $^2H, ^3H$ ) mixture are heated within short-term cycles ( $\tau = 10^{-8}$  sec) by a dynamic powerful electron and laser beams so as to trigger a micro-nuclear explosion at ultrahigh pressures;
- quasi-stationary systems (Tokamaks), in which such mixtures are heated to a plasma state and held for periods  $\tau < 1$  sec by strong magnetic fields at low pressure and ultrahigh temperature  $t > 10^8 \div 10^9$ °C.

The resolution of the problems relating to thermonuclear power installations can be (**Figure 1**) divided into three main stages:

- the creation and use of research reactors (1960–2000);
- the creation of demonstration reactors with a positive energy yield (2000–2030);
- the anticipated creation of industrial reactors producing energy on an industrial scale in thermonuclear power plants (2050–2100).

In Russia, the first stage included a pulsed thermonuclear installation of the first type, Angara-5 (**Figure 2**) in which a micro-fusion explosion was triggered by a stream of electrons emitted from a system of super-powerful condensers, and a series of fusion reactor installations of the second, or tokamak type (T-7, T-10, T-15, T-20).

The emergence and behavior of thermonuclear fusion of a deuterium-tritium mixture with the formation of helium occurs in Tokamak installations, with the release of high energy. Maintaining this reaction in the toroidal chamber is carried out by a powerful alternating magnetic field generated by the network of coils. The thermonuclear fusion reaction is carried out in the plasma inside the chamber, heated to a temperature of over 100 million degrees. Huge mechanical and thermal forces arise in electromagnetic coils with a superconductor at cryogenic temperatures. These forces generate high stresses and strains in Tokamak structures (**Figure 3**).

Drawing on research into all types of reactors [4–10] on the basis of the above developments of experimental thermonuclear installations, in 1995 an international work (USA, USSR-Russia, Japan, India, France, South Korea and others) began on the development [3, 11, 12] of the world's largest international demonstration thermonuclear



**Figure 2.**  
*Angara-5.*

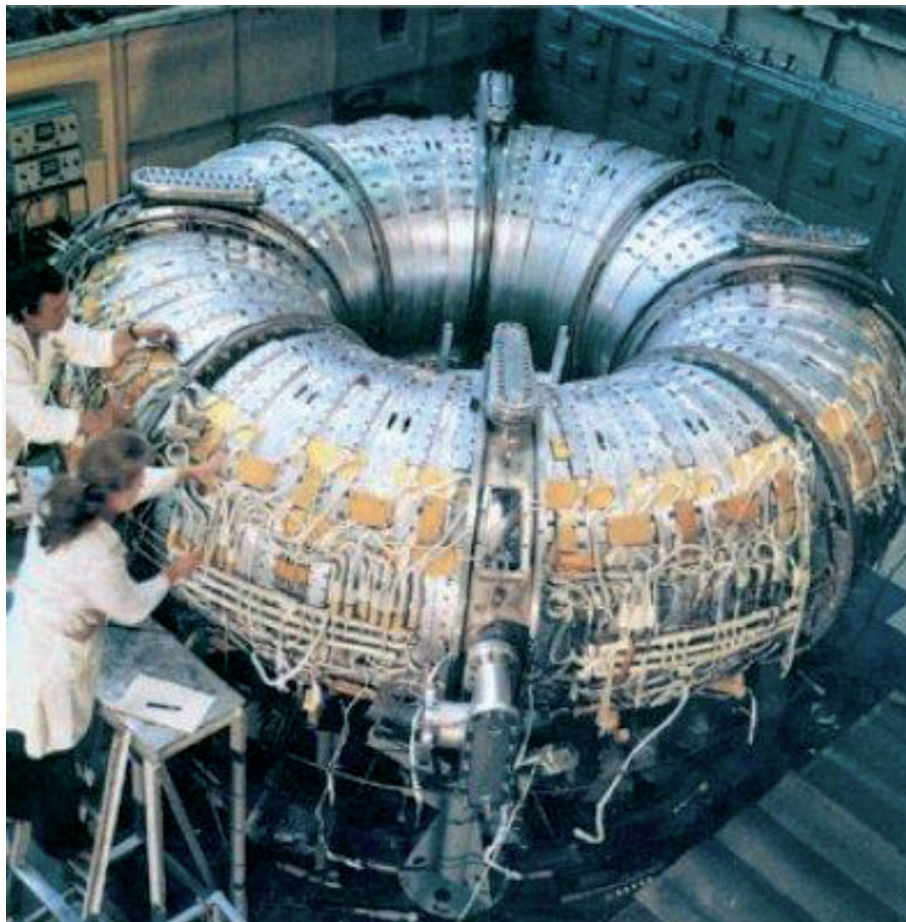


**Figure 3.**  
*Tokamak T-7.*



**Figure 4.**  
*International thermonuclear experimental reactor ITER (ITER).*

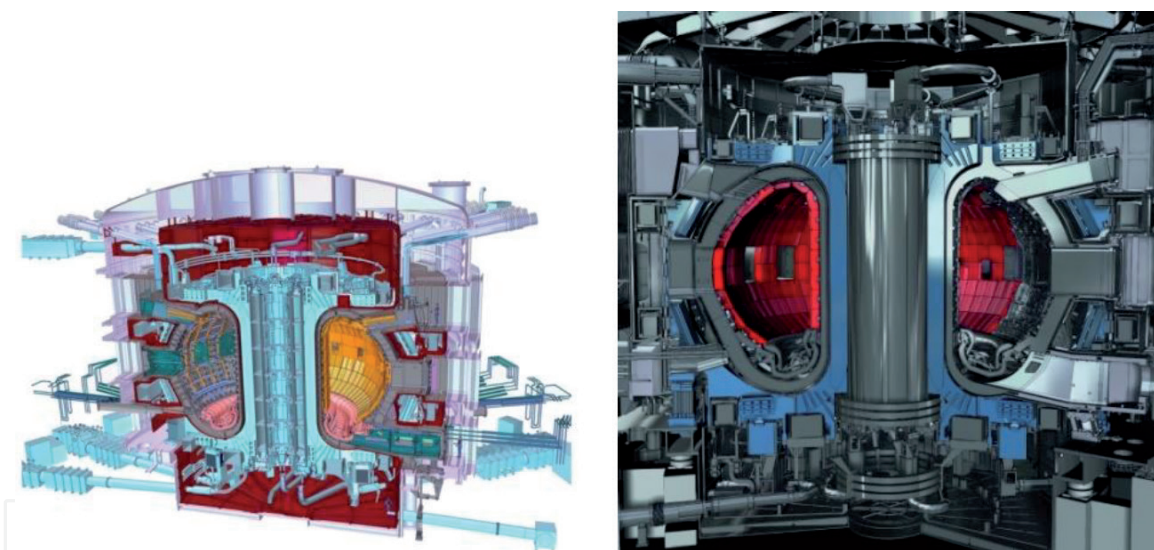


**Figure 5.**  
*Schematic diagram of the international thermonuclear experimental reactor ITER.*

reactor, or ITER (**Figure 4**) with a chamber volume of  $830 \text{ m}^3$  and a plasma temperature of  $100\text{--}500$  million  $^{\circ}\text{C}$  (**Figure 4**), to be completed by 2025 (**Figure 5**).

## 2. Analysis of special operating conditions and limit states

Experimental thermonuclear reactors of the tokamak type are fundamentally different from the nuclear power plants (NPPs) using tested thermal and fast neutron [4] technology that is currently in operation. These specific features of the experimental reactors include:

- a wide range of low operating temperatures,  $t$ , from room temperature of  $t = + 20^{\circ}\text{C}$  to cryogenic temperature of  $-269^{\circ}\text{C}$  (liquid helium temperature) in superconducting systems of electromagnetic coils for the creation of magnetic fields;

- high temperatures (up to  $+800 \div 1000^{\circ}\text{C}$ ) on the working walls of the chamber and ultra-high temperatures (up to  $+100000000^{\circ}\text{C}$ ) in the plasma;
- ultra-high magnetic fields  $M$  for holding and controlling plasma from 3 to 20 Tesla (T);
- controlled electromagnetic fields of unstable duration  $\tau$ , with a frequency of change  $f$  of up to 1000 Hz;
- extremely high mechanical  $Q_M(\tau)$ , thermal  $Q_t(\tau)$  and  $Q_{em}(\tau)$ , electromagnetic forces  $Q_{em}(\tau)$  reaching  $100 \div 1000$  MN;
- ultra-high density,  $i$ , of the electric current in the coil superconductors;
- widely varying mechanical and physical properties (coefficient of thermal expansion  $\alpha$ ), elasticity modules  $E$ , yield stress  $\sigma_y$ , and ultimate strength  $\sigma_u$  of the conjugated structural composite materials (superconducting wires, conductors, coils, support structures, multilayer chamber walls);

The design features and loading conditions, listed by the parameters:  $\tau$ ,  $Q_M$ ,  $Q_t$ ,  $Q_{em}(\tau)$ ,  $t$ ,  $E$ ,  $\sigma_y$ ,  $\sigma_u$ ,  $\alpha$  are combined with standard and emergency situations (for example, loss of superconductivity and contact of plasma with the chamber wall).

When justifying the strength of load-bearing structures, the two most important tasks are:

- to determine the stress-strain states in hazardous areas during normal and emergency situations;
- to determine the limit states resulting in high levels of plastic deformation and fracture.

The limit states in the load-bearing structures of the tokamak will be related to:

- the achievement of critical fracture stresses  $\sigma_c$  and strains  $e_c$  under extreme loads  $Q_{max}(\tau)$ ;
- the achievement of maximum permissible strains,  $e_k$ , in superconductors at the stage of loss of superconductivity when the reactor is cooled down to critical helium temperatures and when the maximum electric current  $I_{max}$  with a density  $i_{max}$  is introduced into the superconducting coils;
- the occurrence of critical damage as a result of exposure to a combination of variable mechanical  $Q_m(\tau)$ , electromagnetic  $Q_{em}(\tau)$ , thermal  $Q_t(\tau)$  and contact  $Q_k(\tau)$  forces.

The above are the basic parameters for determining the local stresses,  $\sigma$ , the strains  $e$ , strength and service life of a thermonuclear installation [6].

$$\{\sigma, e\} = F\{Q(\tau), E, \mu, \tau, t, S\} \quad (1)$$

$$\sigma_{max} \leq \left\{ \frac{\sigma_y}{n_y}, \frac{\sigma_u}{n_u} \right\} \quad (2)$$

$$\tau \leq \frac{\tau_c}{n_\tau}, N \leq \frac{N_c}{n_N} \quad (3)$$

where  $F_\sigma$  is functional,  $S$  is the characteristic of the dangerous section,  $\sigma_{\max}$  is the maximum stress at the critical point of the dangerous section,  $n_y$ ,  $n_u$  are safety factors for yield stress and ultimate strength,  $\tau_c$ ,  $N_c$  is the critical time until fracture (service life) and  $n_\tau$ ,  $n_N$  safety factors for service life.

For thermonuclear installations  $n_y < n_u < n_\tau \approx n_N$ .

The creation of energy-efficient and safe thermonuclear tokamak installations is largely dependent on the successful solution of the problems of deformation and fracture mechanics.

A characteristic feature of large tokamaks as mechanical systems is the presence of significant ponderomotive loads  $Q_{em}(\tau)$ , which act in combination with the special operating conditions in the main systems of the installation - the electromagnetic system (EMS) for plasma confinement and the discharge chamber.

The electromagnetic systems used in tokamaks give rise to high and ultrahigh forces  $Q(\tau)$ , which results in high mechanical stress on the structural elements. Moreover, in superconducting EMS, structural, current-carrying and insulating materials operate at cryogenic temperatures (down to 4.2 K), which affect the physical and mechanical properties of these materials. The discharge chambers of tokamaks are exposed to complex mechanical, thermal, and radiation loads.

One specific feature of tokamaks is that they operate in an alternating programmed stable and unstable mode, and so their power elements are subject to cyclic loads. The calculation and design of such elements needs to be carried out based on their actual operational characteristics, using an apparatus with static, dynamic and cyclic strength and taking into account plastic deformation of the materials.

The program of research into controlled thermonuclear fusion technology provides for an increase in the size and intensity of magnetic fields and more complex operating conditions of tokamak coils. Moreover, the standards in relation to the durability, rigidity, and reliability of load-bearing elements are also increasing, which will ensure that the required physical parameters are complied with in respect of the facilities. There is therefore a pressing need to consolidate the expertise in solving problems related to mechanics, durability, service life and safety issues which has been accumulated during the development of the tokamaks used in the largest thermonuclear installations. In Russia, these were the T-15 tokamak and the Strong Field Tokamak (SFT) installations.

### 3. Experimental study of stress-strain states

Computational and experimental studies of the deformation fields of a structure make it possible to determine the relationship between the levels of stress-strain fields in hazardous zones of the structure which are inaccessible for direct experimental research, and in areas which are accessible for the purpose of continuous observation. The determination of these functional dependencies forms the experimental and theoretical basis for monitoring the operational performance of the installations.

The main stages of research into the stresses to which the critical elements of power installations are exposed include:

- an analysis of the initial data on -magnetic fields, ponderomotive loads and boundary conditions which is necessary for research using models, full-scale elements and mathematical calculations;

- the development of algorithms and programs to perform mathematical calculations and process of experimental results;
- the theoretical optimization of the design parameters;
- the development of methods and instruments to measure deformations in cryogenic conditions and strong magnetic fields;
- the development of systems for full-scale measurement of strain at the main nodes of the installations;
- testing of materials to determine basic design characteristics;
- research on various types of model - photo-elastic, low-modulus, and models using strain-sensitive coatings;
- full-scale inspection of the main components of installations in operational conditions and near-operational conditions, for strain measurement purposes;
- analysis of the results in order to assess strength and service life of the structure.

Below are some of the main results of the research on the T-15 installations.

The T-15 installation is designed to create and study plasma with parameters that are close to the thermonuclear level and are sufficient for a reliable transition to the plasma state. One of the main technical features of the T-15 installation is the use of superconducting toroidal field coil (STFC).

Each coil unit contains coils of a superconducting current-carrying components, enclosed in a rigid steel case. The coil is a transversally isotropic ring made of a complex composite material consisting of a niobium-tin superconductor in a copper matrix, insulating materials and channels for a coolant (helium).

The T-15 unit contains 24 STFC units located around the central support cylinder along the torus-shaped vacuum chamber. A structural diagram of the SCTF unit is shown in **Figure 6**.

It has been established that as a result of the interaction of the STFC currents with the toroidal and poloidal magnetic fields in the STFC units, two types of volumetric ponderomotive loads arise:

- toroidal static forces acting in the plane of the STFC unit. The resultant force of this load is directed towards the center of the installation;
- poloidal impulse forces acting on the coil perpendicular to the its plane. These lateral forces create a tilting moment relative to horizontal diameter of the coil.

For the purposes of the operation of the T-15 unit, provision is made for nominal and forced modes with and without disruption by plasma current. The values of the loads acting on one unit are shown in **Table 1**.

The maximum strain of a superconductor in any mode may not exceed 0.2%, since the current-carrying capacity of superconducting systems (SCS) drops sharply at strains of more than 0.5%.

Due to the symmetry of structure and loads, all STFC units are subject to the same conditions. Therefore the calculation and experimental study of their

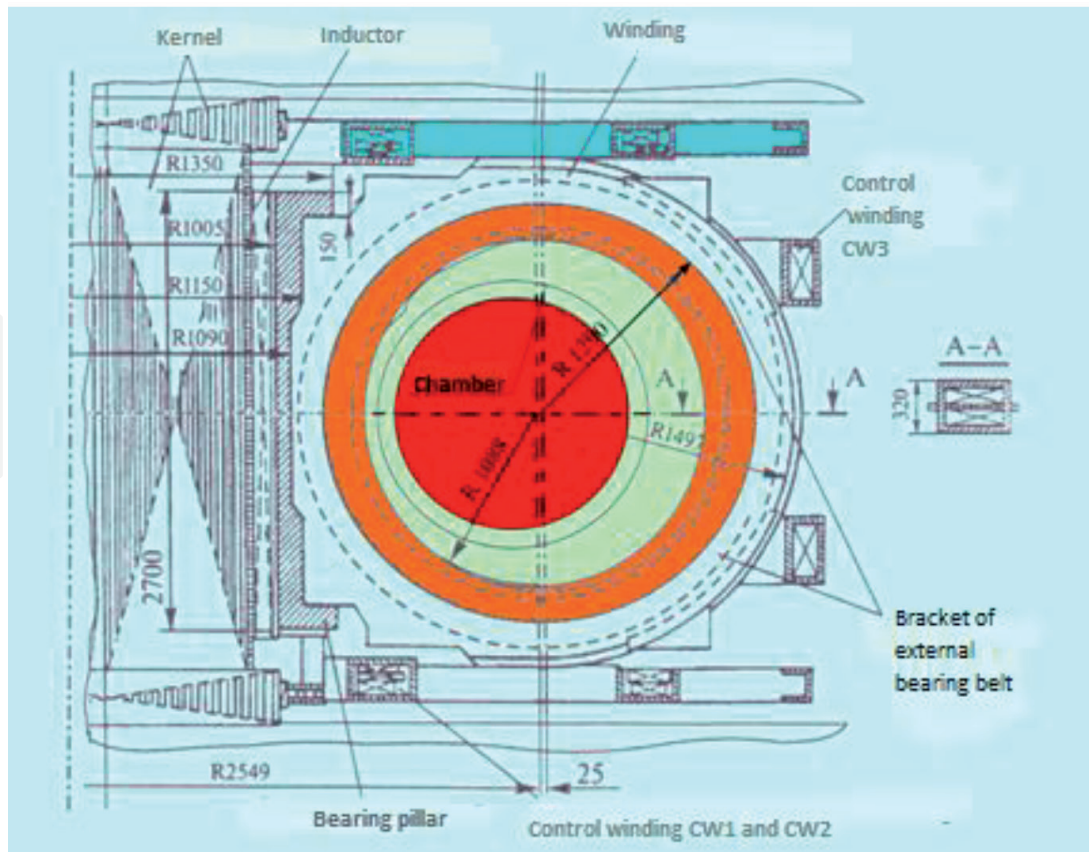


**Figure 6.**  
 Structural diagram of the STFC unit.

T-15 operation mode	Central force, MN	Overturning moment, MN · m	Number of loading cycles
Nominal:			
without disruption	6.07	1.45	80,000
with disruption	6.07	2.4	400
Forced:			
without disruption	12.4	2.17	20,000
with disruption	12.4	3.6	100

**Table 1.**  
 Loads acting on the unit.

stress-strain state (SSS) is carried out taking into account the corresponding symmetry and support cylinder conditions.

To study the effects  $Q(\tau)$  of stresses  $\sigma(\tau)$  and strains  $\epsilon(\tau)$  associated with the action of magnetic and thermal fields, foil strain gauges with sensitive elements made of constantan and wire (wire diameter  $30 \mu\text{m}$ ) and high-temperature tensoresistors made of a nickel-molybdenum and iron-chromoaluminum alloy were used. The tensoresistors were installed on samples consisting of three materials, simulating the main structural materials of the tokamak: stainless steel, copper alloy and a composite material. As a result of the first series of experiments, it was found that in magnetic fields of 1–3 T the response of the output signals from the strain gauges was  $20 \times 10^{-6}$ , with standard deviations of about  $S = 1.5 \times 10^{-6}$ .

To develop tensoresistors with optimal characteristics at cryogenic temperatures, nickel-molybdenum tensoresistor alloys with a low electrical resistance coefficient in the temperature range of  $-269$  to  $= 20^{\circ}\text{C}$  ( $4\text{--}300 \text{ K}$ ) were created. Under

appropriate heat treatment modes (**Figure 7**) these alloys have a high residual electrical resistance  $K_t$  at ultralow temperatures down to  $0.5 \times 10^{-6} K^{-1}$ .

**Figure 8** shows the layout of the primary converters and the results of the study of stresses during cool-down and the injection of current into the system consisting of two experimental STFC units located side by side and not aligned. With the units arranged in this way, the interaction of their fields creates a load that approximately corresponds to the load on the units in the operating mode. It has been established by measurement that at a cooling rate of up to 3 K/h, the maximum stresses arise at temperatures up to 60 K and do not exceed the yield stress  $\sigma_y$ . With a further decrease in temperature, the level of the stresses decreases, and

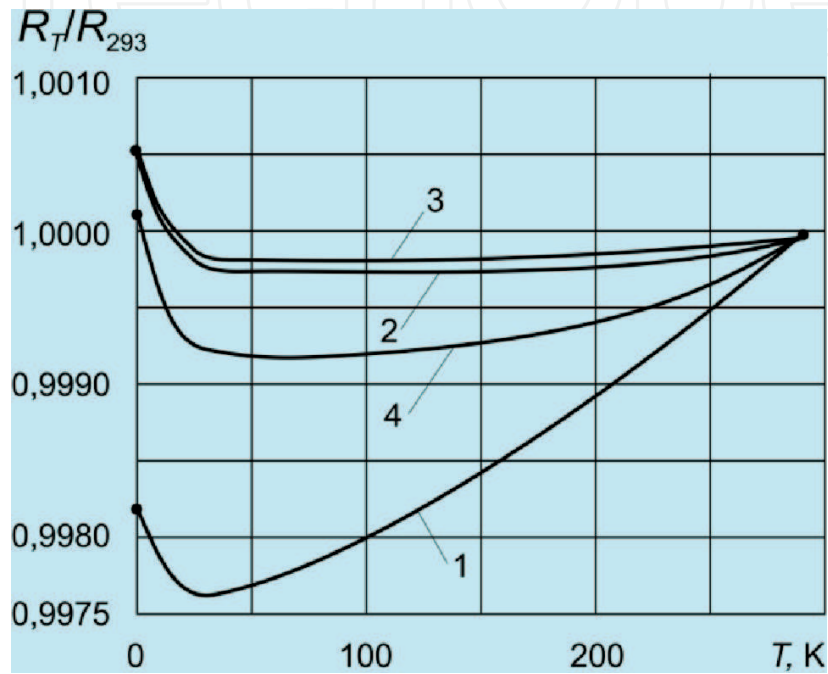


**Figure 7.** Temperature correlation between electrical resistance after quenching and various stabilizing annealing modes (1 - quenching, 2 - quenching and annealing for 30 minutes at a temperature of 470°C, 3 - annealing for 2 hours, 4 - annealing for 5 hours).

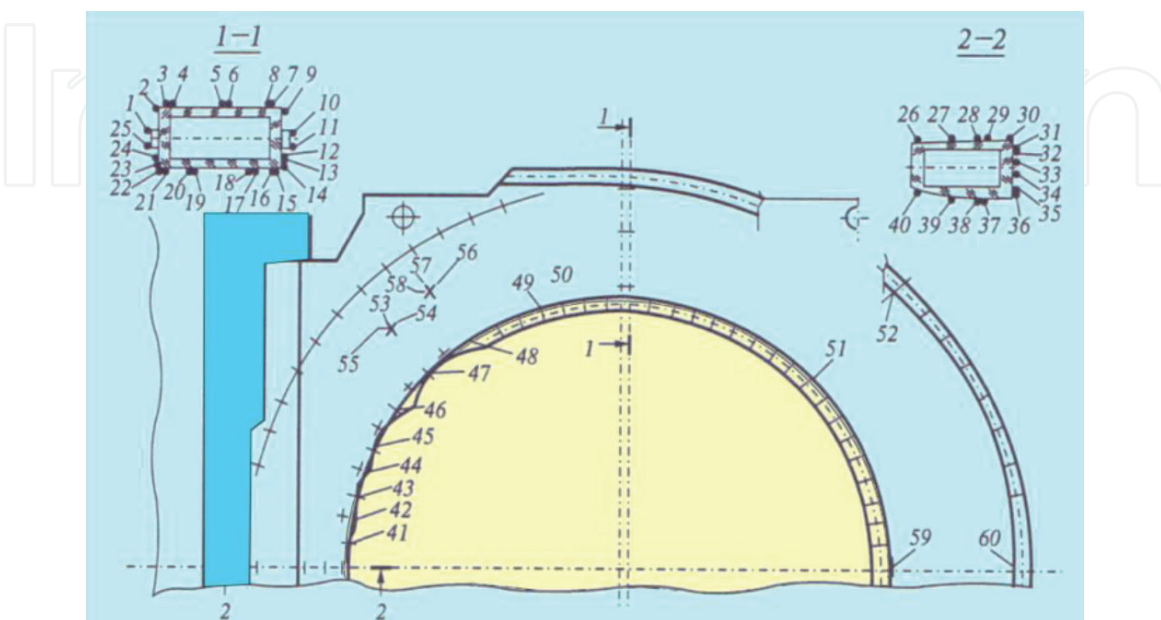


**Figure 8.** Arrangement of tensor resistors on the strain gauge model of the case of the STFC unit in the T-15 installation (the figures refer to the - numbers of the tensor resistors located along the diameter, across and at an angle of 45°).

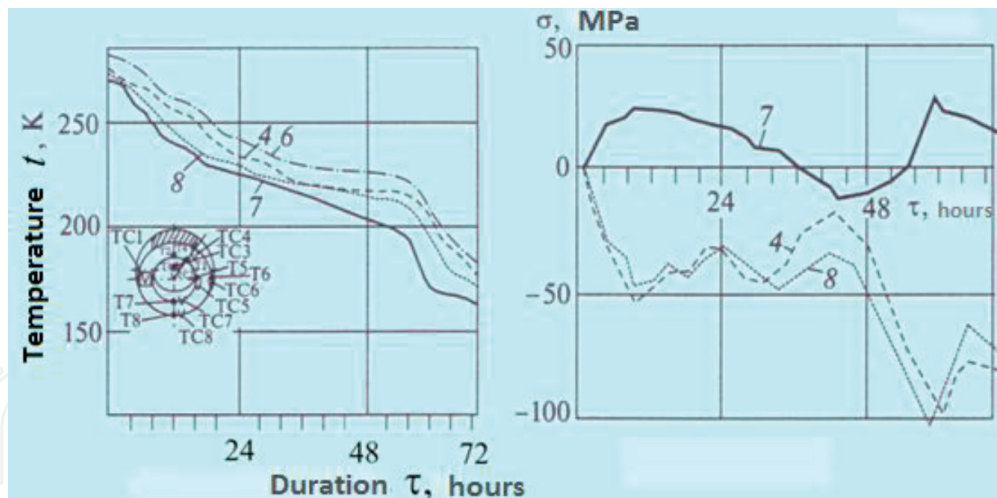


**Figure 9.**  
*Temperature and stresses in the housing of the STFC unit during cool-down.*

the temperature field becomes more uniform. The measurement of displacements of the SCS relative to the body during the initiation of the current revealed shifts of up to 15 mm, which could lead to the delamination of the SCS from the walls of the body. On the basis of these measurements, measures were taken to increase the stiffness of the sealing of the coils in the body of the standard STFC units to ensure their operational fitness.

The results of the temperature  $t(\tau)$  and stress measurements  $\sigma(\tau)$  during cooling are shown in **Figure 9**. The layout of the resistance thermometers, RT, and tensoresistors, T, is shown under the curves.

The numbers of the curves correspond to the numbers of resistance thermometers RT.

Measurement of the changes in stresses when current - from 0 to 15 kA - was introduced into the superconducting systems showed that in the support cylinder the stress reached 110 MPa, and 40 MPa when the discharge chamber was heated.

#### 4. Calculations and physical modeling

The initial computational study of the stress-strain state of the STFC unit as a result of the action of toroidal forces in a complete setting provides a solution to the spatial problem. By using equivalent elasticity modules and taking into account the nature of the load, this problem can be restated more simply, in two dimensions. The nature of the SSS in radial sections of the STFC, which are remote from the support column, can be investigated in an axisymmetric setting. The SCS coil housed in the steel power case of the STFC is anisotropic in the circumferential and radial directions. These problems can be solved using the finite element method.

At the initial design stage, calculations were carried out in order to select the best design option. Then, for the selected design option, a study of the stress-strain state of the STFC unit was carried out in relation to the refined design schemes using the finite element method and physical modeling, which allows specific features of the design to be taken more fully into account.

The influence of the following factors was studied:

- the bending stiffness of the support cylinder;
- the radial technological gap between the STFC units and the support cylinder;

- the volumetric nature of the application of loads and the force interaction between the case and the SCS coil;
- the anisotropy of the coil properties.

The superconducting toroidal field coil (STFC) has a strong anisotropy in respect of its mechanical and thermophysical properties. On the planes adjacent to the strips separating the half-shells, contact friction arises during each pulse, which in cryogenic conditions is undesirable from the point of view of heat release and insulation integrity. The ponderomotive forces which compressing the STFC in the radial direction and stretching it in the circumferential direction during each pulse cause gaps to appear between it and the body bandaging it. The significant lack of uniformity in the mechanical and thermophysical properties of the SCS causes a significant lack of uniformity in the stresses to which it is subject, which can lead to appearance of plastic deformations and accumulation of residual stresses in the SCS.

The modeling of strains and stresses in the SCS was carried out using polarization and optical methods.

The calculations of the SSS of the STFC unit, taking into account all the above factors, are shown in **Figure 10**.

In order to ensure that the electrical insulation is reliable, the contact interaction at the node where the support column is connected with a pin to the metal-polymer coils of the STFC (see **Figure 6**) needs to be calculated and assessed. The stress state of the node is almost flat and skew-symmetric. The initial contact takes place near the corner point (**Figure 11a**). At this point of contact, the stresses are very high, which may lead to destruction of the polymer coating. The simplest stress-limiting change in a contact surface is the - rounding of a sharp edge. However, the stress distribution remains significantly uneven (**Figure 11c**), with a sharp increase in stresses near the rounded edge at point A. Analysis of similar options for the contact interaction between a rigid punch and an elastic layer shows that a more favorable pressure distribution takes place when the punch is convex in shape, in which case the curve on the diagram is close to parabolic, with zero pressures at the boundary of the contact area (**Figure 11c**).

The determination of the SSS of the STFC unit resulting from the action of poloidal forces,  $Q$ , - is a complex spatial problem involving the mechanics of a

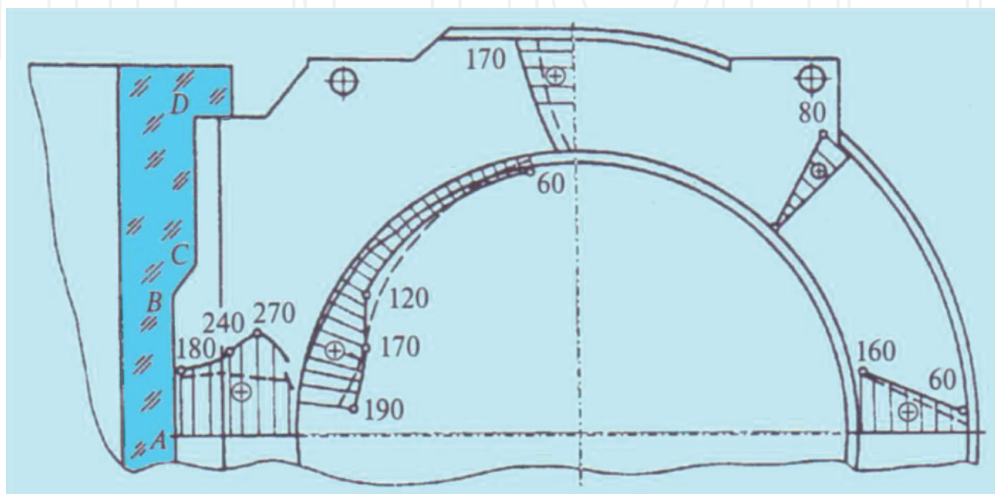


**Figure 10.**

*Circumferential stresses in the unit body when it is supported by the column along the AB line; solid lines (-) - values reached by experiment; dotted lines (--) - calculated values.*

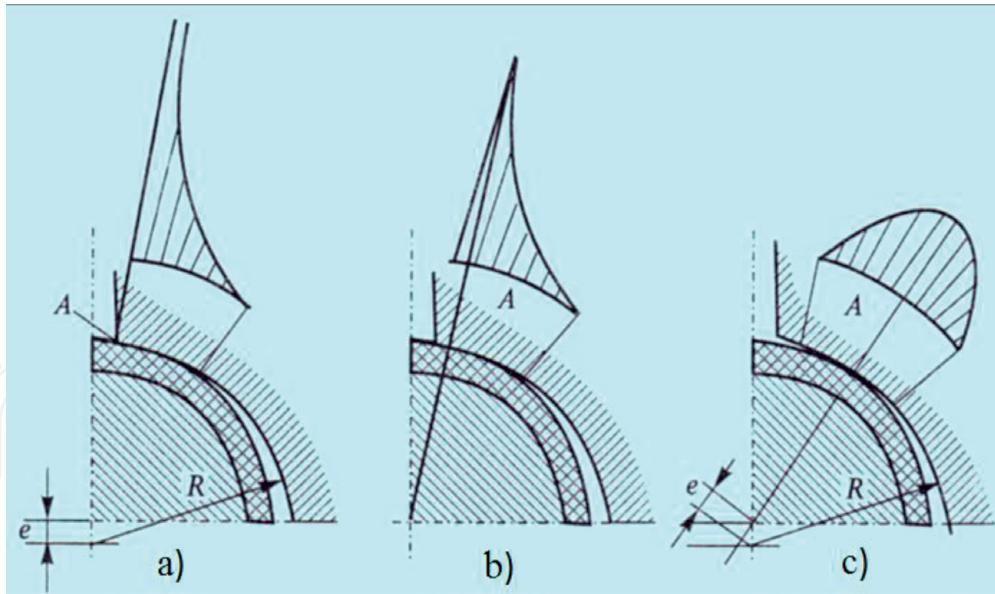


**Figure 11.**  
 Distributions of contact pressures on a metal-polymer pin with various hole shapes and a split support column with a sharp (a) and rounded (b) edge and (c) with a displacement of the point of initial contact A.

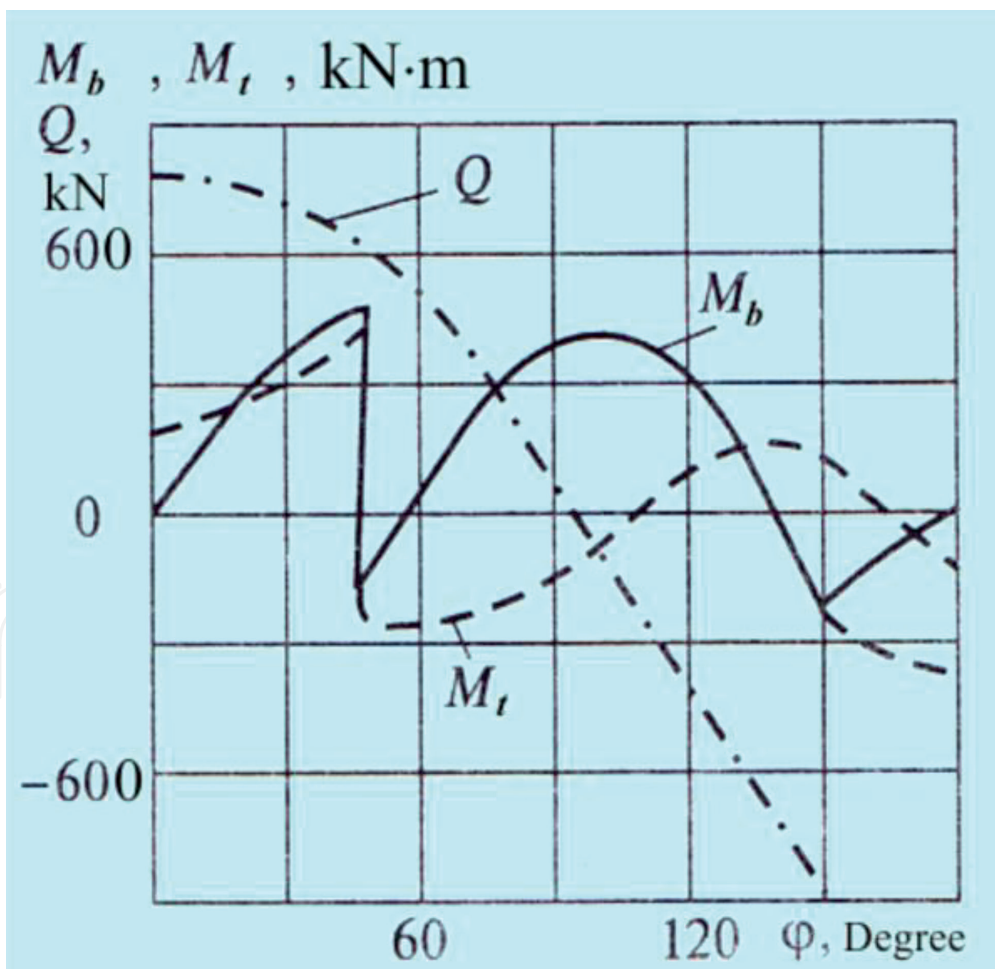


**Figure 12.**  
 Distributions of bending and torque moments and shearing forces arising in the forced mode when the plasma current is disrupted.

deformable solid body. This task was solved using a pivotal approach. To determine the SSS, the rod theory is used: this theory takes into account the potential energy of bending, torsion and antiplane shear deformations. A rod is viewed as an elastic

curve with bending, torsional and shear stiffness. Since the stiffness of an SCS coil with such indicated deformations is low, compared to the stiffness of the unit body, the former can be ignored, thus increasing the design safety margin. The calculation is performed using the force method. The calculation results for the forced mode, in the form of distributions of bending and torque moments and shearing forces, with a disruption of the plasma current when these loads are at a maximum, are shown in **Figure 12**.

## **5. Design analysis of local stresses in composite structures of the reactor**

The intra-chamber components of thermonuclear reactors, including ITER [3, 6, 11, 12], are subject to high stress levels, and are the most critical elements as they are in direct contact with the plasma. Taking into account p. 2, they are designed to withstand cyclic loads resulting from intense heat flows and volume forces, thermal shocks and dynamic effects during plasma disruptions and abrupt displacements of magnetic axes. The operating conditions to which the materials used are subjected are complicated by exposure to radiation.

When designing intra-chamber components, it is very difficult to find a structural material that is sufficiently resistant to all the above factors simultaneously and can provide the structure with the required operability and service life. The intra-chamber components were therefore constructed using layers of materials with different qualities: beryllium, copper, stainless and austenitic steel.

In view of the high stresses to which the individual layers whose surface is directly in contact with the plasma, are exposed, and their increased brittleness, it is of great importance to apply fracture mechanics methods in order to confirm and ensure their integrity.

The main load factor to which the multilayer elements of the first wall are exposed is the effect of plasma in the form of cyclically repeating high power heat flows and changing electromagnetic loads during plasma disruptions. Design strength analysis needs to be conducted in respect of such elements, taking into account possible changes in their properties during heating and increased brittleness due to radiation [4–8, 11, 13].

In addition to thermal loads caused by varying temperature fields, areas adjacent to the boundaries of the composite layers experience additional loads due to the difference in the thermal expansion coefficients of the dissimilar materials. Moreover, residual stresses caused by the manufacturing process are localized in this area. Due to differences in the materials' physical and mechanical properties, these residual stresses are not relieved during subsequent operational heating.

In effect, the boundary between the layers can be considered as another material, with own initial level of damage and defects, and a specific fracture resistance. For example, one of the problems with obtaining efficient Be/Cu compounds was that combining beryllium with almost any other material results in the formation of brittle intermetallic phases [5, 14, 15].

The operating conditions to which the dissimilar materials used for the structure are subjected are complicated by exposure to radiation, which increases the likelihood of fracture due to brittleness. The fracture resistances of the materials used (beryllium, copper and stainless steel), taking into account increased brittleness due to radiation, are set out in the report [16].

To maintain the proper operational condition of the multilayer element which is in contact with the plasma, it is necessary to ensure both the integrity of the reinforcing material (beryllium) and the proper operational condition of the beryllium-copper joint. Possible damage (failure) scenarios during operation

include the initiation of a brittle fracture in the beryllium layer, and delamination at the beryllium-copper boundary.

For the purpose of assessing the damage resistance of a heterogeneous structure, it can be divided into three separate zones: areas remote from the boundary between layers of dissimilar materials; areas near the boundary; and the boundary itself.

To assess the fracture resistance of layers remote from the boundary, fracture mechanics appropriate to a homogeneous material can be applied. The applicable theoretical and practical foundations applicable to this case have been developed [17, 18].

To analyze the resistance to brittle fracture of the materials in the layers located near the boundaries, the methodology appropriate for a homogeneous material is applied, but the corresponding analytical formulae for calculating the criterion parameters need to be adjusted [19]. This applies to the boundary zone where dissimilar materials are joined together, which is, at present, the area in respect of which least research has been done.

The main factors to be considered are as follows.

- The boundary between dissimilar materials forming a junction are sources of stress and strain singularities. This applies both to cracks occurring at the boundaries between dissimilar materials (delamination cracks), and to the points where the boundaries between materials exit to a free surface.
- In order to calculate the stress-strain state (SSS) in such singular zones using modern mathematical methods, special finite elements need to be developed whose shape functions allow the features of the SSS in the zones of crack tips or corner points, as well as in their immediate vicinity, to be taken into account [20, 21].
- The materials used in multilayer elements do not have levels of fracture resistance: copper is prone to radiation embrittlement and beryllium is a fragile material. The durability and fracture resistance characteristics of laminated structures largely depend on the technology used in their manufacture.

In view of the above, in accordance with currently accepted design practice the calculation of the durability of multilayer elements in reactors needs to be carried out in two stages.

1. The first stage is the assessment of strength of multilayer elements without taking into account the singular zones and possible fractures, which can be performed on the basis of classic criterion-based approaches, taking into account the known characteristics of the materials used in a multilayer composition. In doing this, modern methods of mathematical modeling need to be used to analyze the SSS under power and temperature loads.
2. The second stage is the calculation of structural elements using fracture mechanics methods, taking into account the special characteristics of the SSS in singular zones (strains) and postulated crack-like defects, in order to assess safety coefficients while taking brittle fracture into account.

In the case (**Figure 13**) of a homogeneous plate with a fracture  $l$  under nominal loads  $\sigma$  [5–8, 17–20, 22] the distribution of local stresses  $\sigma_r$  at a distance  $r$  from the crack tip is described by a singular equation:

$$\sigma_r = \frac{K_I}{\sqrt{\pi r}} \cdot f_k = \left( \frac{K_I}{\sqrt{\pi}} \cdot f_k \right) r^{-\lambda} \quad (4)$$

where  $K_I$  is stress intensity factor of at the crack tip ( $K_I = \sqrt{\pi l}$ ),  $f_k$  is a dimensionless function, which depends on the dimensions of the plate and crack, and  $\lambda$  is the singularity index ( $\gamma = -0.5$ ).

In accordance with the strength conditions (1) and (2) for a plate without a fracture ( $l = 0$ ) and where a fracture is present as shown in **Figure 12**, the fracture resistance condition is written in the form

$$K_I \leq \frac{K_{Ic}}{n_k} \quad (5)$$

where  $K_{Ic}$  is the critical stress intensity factor and  $n_k$  is safety factor for fracture resistance ( $n_k \leq n_u$ ).

During the analysis of the design features of the multilayer elements of the first wall of the thermonuclear reactor [14, 23, 24] several main types of singularity sources were identified (**Figure 14**):

- singularities resulting from including in the calculation postulated defects (fractures) located in a homogeneous layer of a multilayer composition (**Figure 14a**);
- a delamination fracture located at the boundary between dissimilar materials (**Figure 14b**);
- a fracture adjacent to the joint boundary (**Figure 14c**);
- joints of dissimilar materials: beryllium-bronze  $90^\circ - 90^\circ$  and  $90^\circ - 180^\circ$  (**Figure 14d, e**).

In a situation as per scheme 14a, in which a fracture (discontinuity) is completely located in one of the homogeneous materials of a multilayer element,

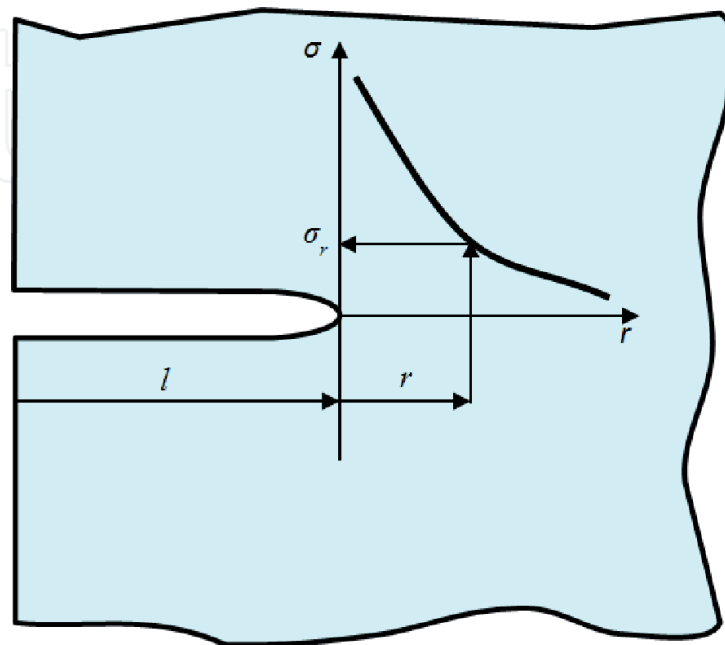


**Figure 13.** Calculation method for analyzing the distribution of stresses  $\sigma_r$  in the crack zone in conditions of plate tension.

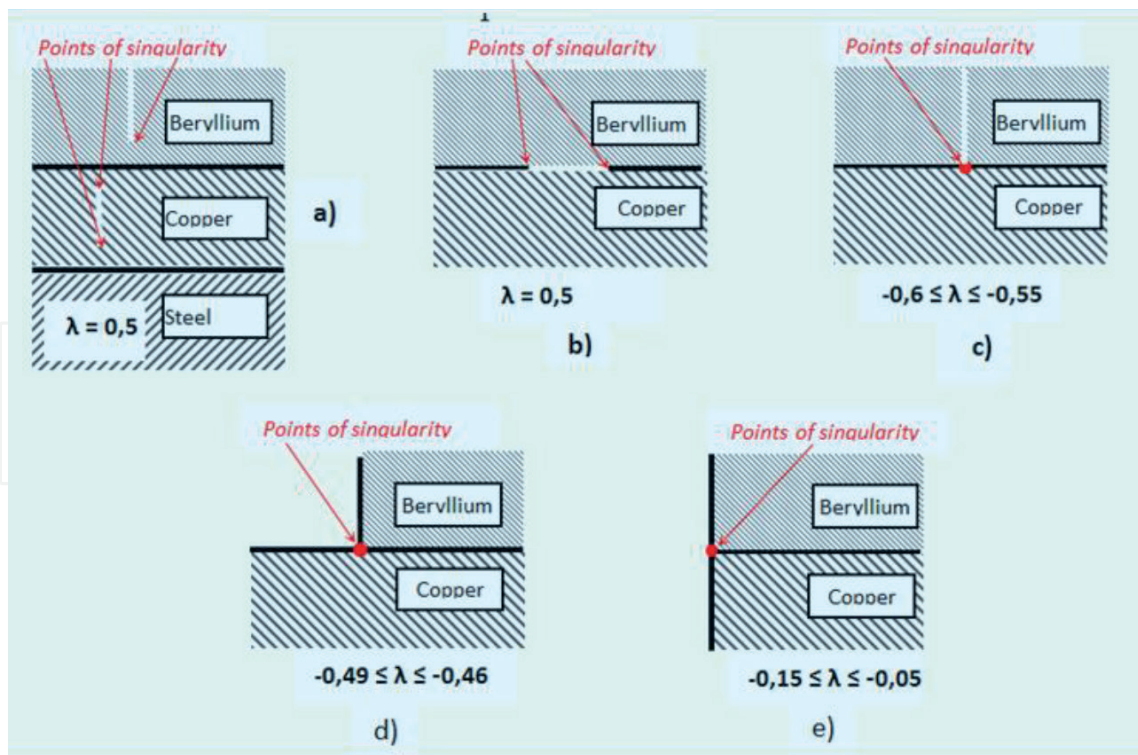


**Figure 14.** Basic types of sources of stress singularities in multi-layer elements of the first wall of reactor. (a) defects (cracks), located in homogeneous material; (b) delamination crack, located at the boundary of heterogeneous materials; (c) crack, abutting on the boundary of a joint; (d) joints of heterogeneous materials Beryllium-Copper 90°-90°; (e) joints of heterogeneous materials Beryllium-Copper 90°-180°.

the procedures for calculating the SSS and durability are well developed ([17, 18, 22]). The level of stress singularity indicator in this case is  $\lambda = -0.5$ .

For delamination fractures (**Figure 14b**), subject to loads by the mechanisms of normal separation and transverse shear, the characteristic Eq. (4), corresponding to the solution of the characteristic equation that determines the degree of stress singularity -  $\lambda$  has a complex root [17, 19, 25].

$$\lambda = -1/2 \pm \beta; \beta = \frac{1}{2\pi} \ln \left( \frac{\mu_1 + \mu_2 \kappa_1}{\mu_2 + \mu_1 \kappa_2} \right) \quad (6)$$

where  $\mu$  is the shear modulus of the materials,  $\kappa = 3-4\nu$  (for plane deformation),  $\nu$  is Poisson's ratio and the indices 1 and 2 indicate whether the material is the 1st or 2nd in the compound of dissimilar materials.

- defects (cracks), located in homogeneous material (**Figure 14a**);
- delamination crack, located at the boundary of heterogeneous materials (**Figure 14b**);
- crack, abutting on the boundary of a joint (**Figure 14c**);
- joints of heterogeneous materials Beryllium-Copper 90°-90° и 90°-180° (**Figure 14c, d**).

From (4)–(6) it follows that the asymptotic distribution of stresses at the fracture tip at  $r \rightarrow 0$ ,  $\beta \neq 0$  is singular, with a different  $\lambda$  singularity. In a bulk (three-component) stress state, three models of fracture mechanics (I, II, III) are introduced into the calculation [18–20], and then, based on (4)

$$\sigma_r = \frac{K_I}{\sqrt{\pi}} \cdot f_{KI} r^{\lambda_I} + \frac{K_{II}}{\sqrt{\pi}} \cdot f_{KII} r^{\lambda_{II}} + \frac{K_{III}}{\sqrt{\pi}} \cdot f_{KIII} r^{\lambda_{III}} \quad (7)$$

The proposed approach to assessing strength of adapters will require additional study of residual technological stresses, which, due to the difference between the physical and mechanical properties of adapter materials, always reach significant magnitudes.

## 6. Strength and durability analysis

Measurement of the changes in stresses  $\Delta\sigma$  when electric current - from 0 to 15 kA - was introduced into the superconducting systems showed that in the support cylinder the stress reached 110 MPa, and 40 MPa when the discharge chamber was heated. During the experimental testing and operation, the elements of the discharge chambers of tokamaks are exposed to mechanical  $Q_m(\tau)$ , temperature  $Q_t(\tau)$  and electromechanical  $Q_{em}(\tau)$  loads, some of which cause the presence of repeated elastoplastic deformations in the areas of stress concentration. As a result, it was necessary to study and substantiate the static and cyclic strength, for which a series of experimental studies was carried out involving the single-frequency and dual-frequency loading of austenitic chromium-nickel stainless steel at a wide temperature range  $t$  from  $-196^\circ\text{C}$  up to  $400^\circ\text{C}$ . The resulting characteristics of the material's resistance to static and cyclic deformation and destruction are an integral part of the general design justification in relation to the strength and durability of the  $N$  elements of the discharge chamber.

The calculations and tests were carried out in relation to the tokamak installation in the presence of a strong magnetic field, the purpose of which was to conduct a physical experiment to study the behavior of plasma under conditions close to those of thermonuclear ignition at minimal technical and economic costs. The use of strong magnetic fields to confine plasma makes it possible to significantly reduce the size of the electromagnetic system of the tokamak and the amount of energy stored in it, and the use of combined adiabatic compression - significantly increases the potential of the experiment. However, in order to increase the magnetic field, a number of complex engineering problems need to be solved.

Structurally, the SFT consists of a discharge chamber in the form of a closed torus of noncircular cross-section, along which 32 sections of the toroidal field coil (TFC) are located. The poloidal field coils (PFC) are located outside the TFC. A structural diagram of the electromagnetic system (EMS) is shown in **Figure 15**.

The interaction of TFC currents with toroidal and poloidal fields leads (by analogy with **Figure 12**) to the occurrence of significant ponderomotive forces acting in the TFC plane and overturning moments tending to rotate the TFC section planes around their horizontal axes. The total vertical force,  $Q$ , disrupting the TFC, is equal to 128 MN, the resulting centripetal force is 108 MN, and the magnitude of torque relative to the vertical axis of the installation is 30 MN·m. In addition to the forces caused by the interaction of magnetic fields and currents, significant forces arise in the TFC, which are a consequence of heating of the conductor.

Ensuring strength of the TFC under the influence of these forces is one of the most difficult tasks involved in developing an EMF. Each section of the TFC is made in the form of a single-turn conductor (bus) made of zirconium bronze, placed in a band made of high-strength non-magnetic steel. The TFC sections are interconnected in such a way that, as a result, a closed thick-walled toroidal shell is formed. This structure is capable of handling both azimuthal and centripetal loads.

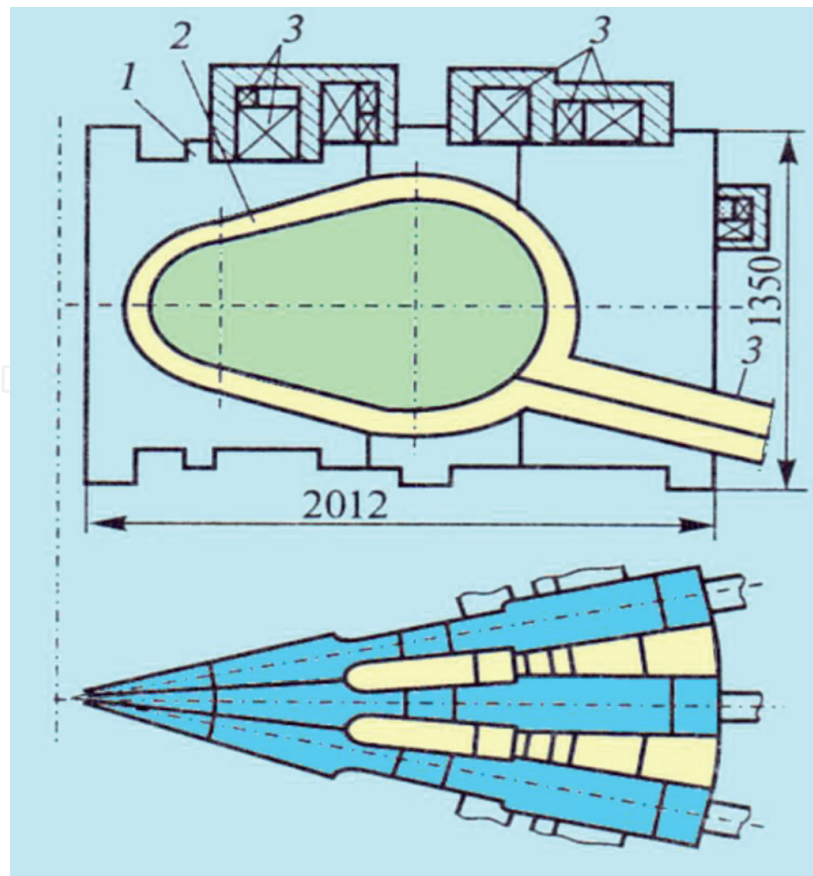


**Figure 15.**  
*Structural diagram of the SFT electromagnetic system. 1 - bandage; 2 - bus; 3 - poloidal field coil.*

It has been established by analysis that it is not possible to solve the problem of ensuring EMS strength by means of traditional safety factors and acceptable stresses. The development of the structure was therefore carried on the basis of the maximum strength characteristics of the material. This approach is acceptable, since the unit is designed for a limited number of impulses.

The selection of the structure of the section, bandage and other load-bearing elements was made by considering the stress-strain state of a number of design options, taking into account the elastoplastic behavior of materials under the action of ponderomotive forces and thermal stresses. The problem of studying the stress-strain state of a structure while a conductor is undergoing elastoplastic deformation can be solved using the finite element method, by applying the theory of plastic flow. Analysis of the stress state has shown that the effect of overturning moments on maximum stresses and strains is insignificant. **Figure 16** shows the distribution of maximum stresses in the TFC unit resulting from the action of ponderomotive forces on the coil in the unit plane, taking into account the heating of the conductor. An assessment of the service life of the EMS has shown that it is able to withstand a given number (1000) of full-scale operating cycles.

The determination of pulse loads on the inner surface of the magnet coil based on the measurements of stresses arising from such loads in individual zones of the structure is an inverse problem of experimental mechanics.

The resolving equation connecting the stresses determined from measurements in a certain zone (**Figure 17a**) with the required load vector on a part of the surface is expressed in the form of a system of Fredholm integral equations of the first kind. It is pointless to attempt to resolve this system - this would be an incorrectly posed problem, -as small perturbations of the initial data can result in arbitrarily large perturbations of the solution. A regularizing algorithm is therefore chosen. The

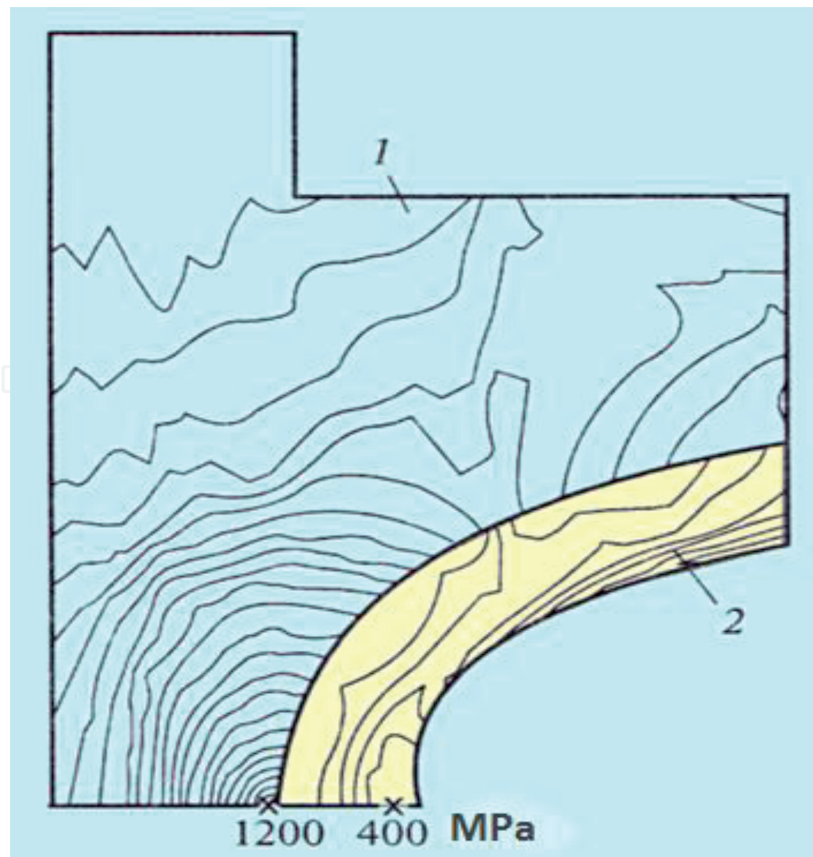


**Figure 16.** Isolines of equivalent stresses acting in the bandage (1) and the bus (2). The asterisks mark the points of local maxima.

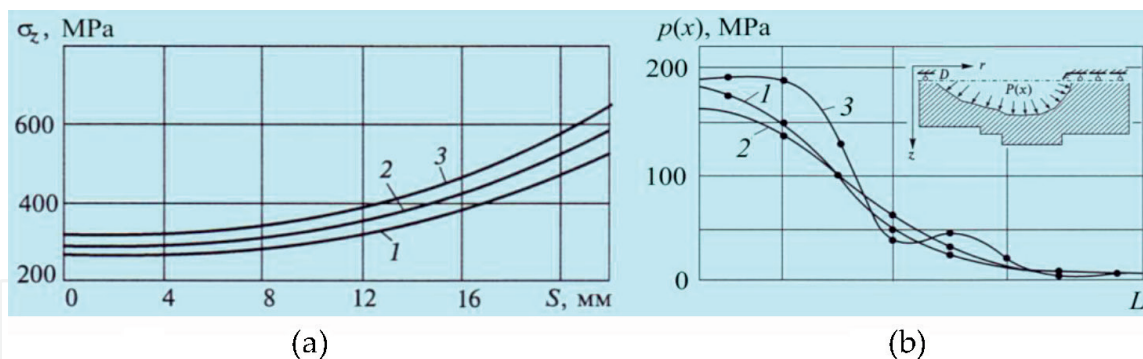


**Figure 17.** The principle stresses in a narrow section of the TFC bandage (a) and the pressure distribution on the wall of the toroidal chamber (b) S - measurement area; L - load area.

restoration of the magnetic pressure in the model was carried out using measurements of strains which were made in a narrow section of the bandage. The measurements of the strains were used to determine the axial stresses in the connector of the toroidal chamber subject to the force of a magnetic field. **Figure 17a** illustrates the axial stresses in the section of the bandage: «these define the error margin (curves 1–3) and are constructed on the basis of experimental data. The corresponding distribution of the magnetic field pressure on the inner contour of the bus is shown in **Figure 17b**, curves 1–3. These results are characterized by a satisfactory level of reconstruction and are consistent with the a priori ideas on the distribution of magnetic pressure.

It is proposed that zirconium bronze be used for the current-carrying elements that are subject to cyclic heating during the operation of the installation. In order to

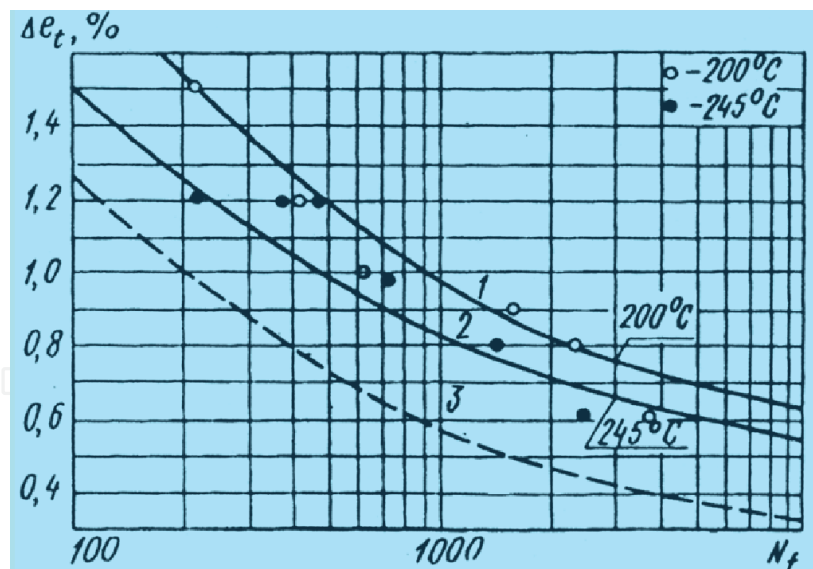


**Figure 18.**  
 Calculated low-cycle fatigue curves and experimental data for zirconium bronze at temperatures of 200 and 245°C.

determine its performance, its resistance to low-cycle deformation and fracture at elevated temperatures was studied.

The calculated low-cycle fatigue curves for zirconium bronze under rigid isothermal cyclic loading are shown in **Figure 18**, in which curve 3 represents the normative equation and characterizes the lower, conservative limit for low-cycle durability, with safety factors for strains  $n_e = 2$  and for durability  $n_N = 10$  [9, 10].

As part of the commissioning work on the creation of SFT, significant emphasis is given to experimental studies of the stress-strain state of the elements of the installation. One specific feature affecting the measurement of strain in the SFT unit is the presence of pulsed magnetic fields of up to 20 T, together with a change in the temperature of the current-carrying elements of up to 250°C and a high level of measured strains (up to 1.2%).

In connection with the impulsive growth of strains and the possibility of the transition of the elements of the wedge part of the bandage and the bus to a plastic state (see **Figures 15** and **16**), it seems possible to use the brittle strain-sensitive coatings method for the purpose of studying the stress fields. Estimates of mechanical stresses in the steel bandage of the model were carried out using the brittle strain-sensitive coatings method at magnetic fields reaching 14 T, with a yield point - of about 12 T.

The analysis and modeling of deformation processes of the elements of a thermonuclear installation in operating mode showed that fretting fatigue arises on the contact surface between the bandage and the bus as a result of the difference in displacements and the presence of contact interactions. This requires special study, since according to [7, 8] it has a significant impact on the installation's integral strength and service life parameters.

As noted above, the characteristics of the mechanical properties of bronze were determined by experiment, using specimens from supplied semi-circular forgings with an average radius of 270 mm and a cross-section of 110 × 140 mm. In order to carry out cyclic tests under conditions that simulate the operation of the busses in contact with the bandage at room temperature, a special loading device was developed that creates a transverse load on the specimen.

When quantifying parameters through the characteristics of the mechanical properties of the studied zirconium bronzes which are included in the Eqs. (1)–(3), this equation takes the form [2–4, 9].

$$e_a = 0,25e_c \cdot N^{-m_p} + 0,435 \frac{S_c}{E} N^{-m_e}, \quad (8)$$

where  $e_c$  is the fracture strain under a monotonic loading,  $m_p = 0.65$ ,  $m_e = 0.06$  are the characteristics of the material.

The value is equal to

$$e_c = \ln \frac{1}{1 - \psi_c}, \quad (9)$$

where  $\psi_c$  is the relative narrowing of the specimen in the neck,  $\psi_c = 0.7 \div 0.75$ .  
Tear fracture resistance at the specimen neck

$$S_c = \sigma_u (1 + 1,4\psi_c), \quad (10)$$

where  $\sigma_u$  is the ultimate strength ( $\sigma_u = 310\text{--}330$  MPa),  
 $E$  is the elasticity modulus ( $E = (1.3 \div 1.5) \cdot 10^5$  MPa).

From the data obtained from service life assessments, taking into account the fretting effect, the amplitude of the fracture strains  $e_a$  in the Eq. (8) needs to be reduced by the reduction factor  $K_k$ . This factor reaches values of 2–2.25.

$$e_{ak} = e_a / K_k \quad (11)$$

which is comparable with the safety factor for durability  $n_e = 2$ , applied in the norms for nuclear reactor calculations [9, 10].

## 7. Conclusions

A combination of various experimental and theoretical studies to determine the load exposure and strength of tokamak installations is an essential foundation for the design of thermonuclear installations, for both demonstration and industrial purposes, and underlies the system of calculations and experiments required in order to actively monitor the stress-strain and limiting states of all load-bearing elements, taking into account the entire range of effects resulting from design, technological and operational factors. The resulting calculations and experimental data on temperature, stress, strain and displacement fields need to be included as initial components in assessments of the strength, service life and survivability of the load-bearing structures of new thermonuclear installations. In general, the research results summarized above demonstrate the correctness of the adopted design solutions, which - in the modes considered during the research - result in a relatively low level of local stresses in the load-bearing elements of the installations. This will contribute [1–3, 6, 23, 24, 26] to improvements in social and economic efficiency and overall safety during the transition from demonstration thermonuclear installations to industrial production, which is anticipated in the second half of the 21st century.

## Acknowledgements

This work was financially supported by the Russian Science Foundation (grant no. 20-19-00769).

IntechOpen

IntechOpen

### **Author details**

Nikolay A. Makhutov, Mikhail M. Gadenin, Sergey V. Maslov, Igor A. Razumovsky  
and Dmitry O. Reznikov\*  
Mechanical Engineering Research Institute, Moscow, Russia

\*Address all correspondence to: [mibsts@mail.ru](mailto:mibsts@mail.ru)

### **IntechOpen**

---

© 2020 The Author(s). Licensee IntechOpen. This chapter is distributed under the terms of the Creative Commons Attribution License (<http://creativecommons.org/licenses/by/3.0>), which permits unrestricted use, distribution, and reproduction in any medium, provided the original work is properly cited. 

## References

- [1] Energy Strategy of the Russian Federation until 2035, Order of the Government of the Russian Federation No. 1523-r, dated 09.06.2020 (in Russian)
- [2] Velikhov E.P., Smirnov V.P. State of research into and future prospects of thermonuclear energy. Herald of the Russian Academy of Sciences. 2006, Volume 76. No. 5. pp. 419-426 (in Russian).
- [3] David Beltran. ITER Electrical Design Handbook. Earthing and Lightning Protection. ITER Technical Report ITR-20-007. The ITER Organization. July 16, 2020. 38 p.
- [4] N.A. Makhutov, M.M. Gadenin, I.A. Razumovskiy, S.V. Maslov, D.O. Reznikov Probability Modeling Taking into Account Nonlinear Processes of a Deformation and Fracture for the Equipment of Nuclear Power Installations. /Combinatorics and Probability. Chapter 8. London. IntechOpen, 2019. pp. 191-220. DOI: <http://dx.doi.org/10.5772/intechopen.88233>
- [5] N.A. Makhutov, K.V. Frolov, Yu.G. Dragunov and others. Risk Analysis and safety improvement in relation to water cooled power reactors. Moscow. Znaniye publ. 2009, 499 p. (in Russian).
- [6] N.A. Makhutov Structural integrity, service life and technogenic safety. Book 2. Novosibirsk: Science publ. 2005. 610 p. (in Russian).
- [7] N.A. Makhutov. Strength, service life, survivability and safety of machines. Moscow. LIBROKOM Publ. 2008. 576 p. (in Russian).
- [8] Problems of strength, technogenic safety and structural materials science Ed. N.A. Makhutov, Yu.G. Matvienko, A.N. Romanov. – Moscow. LENAND publ, 2018. 720 p. (in Russian).
- [9] Standards for calculation of durability of equipment and pipelines of nuclear power installations (PNAE G-7-002-86 - Rules and regulations in the nuclear power industry). Moscow. Energoatomizdat publ. 1989. 525 p. (in Russian).
- [10] Boiler and Pressure Vessel Code. 2010 Edition. NY: ASME. 2011.
- [11] ITER, International Thermonuclear Experimental Reactor. <http://www.iter.org>.
- [12] N.A. Makhutov, M.M. Gadenin. Study of the service life of elements of a thermonuclear power installation, taking into account tribophysics parameters. Mechanics of machinery, mechanisms and materials. 2017. 3 (40). pp. 13-20 (in Russian).
- [13] K. Miya, A. Kobayash, K. Koizumi, K. Hada, T. Shimakawa Construction of structural design guidelines for vacuum vessels and other components. Fusion Engineering and Design. 41. 1998.
- [14] A. Raffray, G. Federici, V. Barabash, H. Pacher, H. Bartels, A. Cardella, R. Jakeman, K. Ioki, G. Janeschitz, R. Parker, R. Tivey, C. Wu. Beryllium application in ITER plasma facing components. Fusion Engineering and Design. 37 ( 2). 1997. pp. 261-286.
- [15] B. Odegard, C. Cadden, N. Yang Beryllium-copper reactivity in an ITER joining environment. Fusion Engineering and Design. 41 (1-4) 1998. pp. 63-71
- [16] F. Moons, R. Chaouadi, J. Puzzolante Fracture behavior of neutron irradiated beryllium. Fusion Engineering and Design. 41 (1-4), 1998. pp. 187-193

[17] G.P.Cherepanov. Methods of Fracture Mechanics: Solid Matter Physics. Springer. 1997. 335 p.

[18] Fracture mechanics and strength of materials. Reference book in 4 volumes. ed. V.V. Panasyuk. Kiev Naukova dumka publ. 1988-1990. (in Russian).

[19] V.D. Kuliev Singular boundary problems. Moscow FIZMATLIT publ. 2005. 719 p. (in Russian).

[20] E.M. Morozov, G.P. Nikishkov The finite element method in fracture mechanics. URSS Publishing house. 2008. 254 p. (in Russian).

[21] S.N. Atluri Computational Methods in the Mechanics of Fracture. North-Holland. 1986. 414 p.

[22] V.Z. Parton, E.M. Morozov Mechanics of Elastic-Plastic Fracture: Fundamentals of Fracture Mechanics. KomKniga publ. 2008. 400 p. (in Russian).

[23] ITER Design Description Document (DDD), G 16 DDD 2 96-11-27 W0.2.

[24] A. Cardella, A. Lodato, H. Pacher, R. Parker, K. Ioki, G. Janeschitz, D. Lousteau, A. Raffray, M. Yamada, C. Gusic. The ITER port limiter design. 43 (1), 1998, pp. 75-92.

[25] M. Williams. The stresses around a fault or crack in dissimilar media. Bull. Seismological Society of America. Bulletin of the Seismological Society of America. 1959. 49 (2). pp. 199-204.

[26] V.D. Kuliev, S.E. Bugaenko, I.A.Razumovsky Development of design criteria for ITER multilayer components. Brittle fracture of multilayer materials. Thermonuclear fusion. Collection of articles. Moscow. NIKIET publ. 1998. (in Russian).